VNU Journal of Science: Natural Sciences and Technology, Vol. 39, No. 4 (2023) 20-28

VNU Journal of Science: Natural Sciences and Technology

Journal homepage: https://js.vnu.edu.vn/NST

Original Article

Zinc Ions Implantation on the Surface of Commercial Papers for Antibacterial and Antifungal Applications

Dao Quang Khai[1,2], Hoang Hieu Chi[1], Nguyen Hoang Duong[2], Nguyen Tam Trong[1], Mai Hong Hanh[1,*]

[1]*VNU University of Science, 334 Nguyen Trai, Thanh Xuan, Hanoi, Vietnam*

[2]*Center for High Technology Development, Vietnam Academy of Science and Technology, 18 Hoang Quoc Viet, Cau Giay, Hanoi, Vietnam*

Received 16 March 2023
Revised 05 July 2023; Accepted 08 July 2023

Abstract: Recently, the demand for novel food-packaging materials with antimicrobial properties has been increasing drastically. In this report, we attempt to implant zinc ions on the surface of commercial paper sheets by using a hydrothermal method to create hydrozincite nanoflake structures. The formation of the hydrozincite nanostructure was attributed to zinc-ion adsorption on the calcite's surface, a common filler used in commercial paper sheets. The zinc-modified paper sheet (PZn) demonstrated a high efficiency to inhibit *C. albicans* and *E. coli* growth. It is attributed to the release of the Zn^{2+} ions into the acidic microbial medium. Along with the eco-friendliness, and biocompatible properties of the paper substrate, the PZn demonstrated a promising application in food packing.

Keywords: Zinc ion, hydrozincite, antifungal, antibacterial.

1. Introduction

Nowadays, food packaging plays a crucial role in our daily lives by protecting food products from contamination and spoilage caused by microorganisms, moisture, ambient air, dust, and mechanical interactions [1, 2]. To address these challenges, developing antibacterial and antifungal packaging materials has garnered significant attention from research teams worldwide [3]. These materials are designed to incorporate agents such as nanomaterials, or metal ions,… that can inhibit or kill microbes, thereby ensuring the safety and quality of packaged food items.

There are many types of polymer films such as polyvinyl chloride, polypropylene, polyethylene-co-vinyl acetate, and polylactic acid have been effectively utilized as a food packing material due to their statical physical and chemical durability [4-6]. Among all natural and synthetic films, cellulose-based membranes are the most appealing. The reason is that cellulose is a particularly common natural polymer, which can be collected from many sources such as wood, cotton,

* Corresponding author.
E-mail address: hanhhongmai@hus.edu.vn

https://doi.org/10.25073/2588-1140/vnunst.5545

microorganisms, or even waste. Moreover, cellulose has some precious characteristics including biocompatibility, recyclability, biodegradability, and eco-friendliness [7]. Recently, many research groups developed antibacterial and antifungal food packing based on cellulose. For instance, the group of Pangye worked on antibacterial and antifungal dialdehyde cellophane, a cellulose derivative [8]. The results have shown that the dialdehyde cellophane had antibacterial and antifungal activity against four gram-positive bacteria, and could well preserve strawberries and tofu. Several recent researches have shown that some metal ions including Ag^{+} [9, 10], Cu^{2+} [11], Ga^{2+} [12], and Zn^{2+} [13] cause different types of microbial cell damage such as membrane degradation, protein dysfunction, and oxidative stress. Among those metal ions, zinc-based compounds containing Zn^{2+} ions were generally acknowledged as a potential metal-based antibacterial and antifungal agent because of their non-toxicity for humans [13], and capacity to inhibit a broad variety of harmful microorganisms [14, 15]. Some research teams have developed antibacterial and antifungal food packing materials from compounds of zinc and cellulose-based films. One of the good examples should be nanocomposite film made of chitosan, carboxymethyl cellulose, and zinc oxide [16], which has antibacterial and antifungal activities. The films were also applied to extend the storage life of white soft cheese. Another noticeable example is the work of Jamileh's team on the reinforcement of polylactic acid films by using zinc sulfide quantum dots and cellulose nanocrystals [17]. The proposed material could hinder the development of *Escherichia coli* (*E. coli*) and was demonstrated as an appropriate candidate for food packing.

In this article, we reported an economical hydrothermal technique for zinc ion implantation on the surface of commercial paper sheets. For determining the optical properties and morphology of the as-synthesized material, we used X-ray diffraction (XRD) patterns, photoluminescence spectroscopy (PL), Raman scattering, and scanning electron microscope (SEM) images. For the antibacterial and antifungal activities application, we examined the antibacterial and antifungal properties of the material towards *E. coli* and *Candida albicans* (*C. albicans*) by using an optical density measurement method.

2. Material and Methods

2.1. Materials

The commercial paper sheets of Double A (1991) PLC were purchased from our local market. Other chemicals including zinc acetate dihydrate $Zn(CH_3COO)_2.2H_2O$ (Merck, >99% purity), ethanol CH_3CH_2OH (Merck, >99% purity), zinc nitrate tetrahydrate $Zn(NO_3)_2.4H_2O$ (Sigma, >99% purity), hexamethylenetetramine $(CH_2)_6N_4$ (Merck, >99% purity), peptone (Himedia), yeast extract (Himedia), meat extract (TM Media), sodium chloride NaCl (GHTECH, ≥99. 5% purity), and glucose (Xilong) were provided with high purity. The microbial strains including *E. coli* and *C. albicans* were achieved from Vietnam Academy of Science and Technology.

2.2. Modified Paper Sheets by Zinc Ion

The hydrothermal method was implemented for zinc ions implantation on a commercial paper sheet. First, a 100 mL solution of ethanol and 5 mM $Zn(CH_3COO)_2.2H_2O$ was prepared. The paper sheet was immersed in the solution for 3 minutes at 60 ℃ before being dried at 70 ℃. These steps were carried out six times. We then put the paper sheets in an enclosed container containing an aqueous solution of 40 mM $(CH_2)_6N_4$ and 40 mM $Zn(NO_3)_2.4H_2O$. The container was maintained at 90 ℃ for 3 hours. Finally, we cleaned the paper sheets with deionized water and allowed them to dry at 70 ℃.

2.3. Optical Investigations

The information about the morphology of the bare paper sheets (denoted by P0) and the zinc-implanted paper sheets (PZn) was seized by a scanning electron microscope (SEM) (FE-SEM s-4800, Hitachi). The size of the

nanostructures was then measured by using Image J. We used a photoluminescence (PL) setup in which the samples were excited by a 325 nm He-Cd laser (Kimmon), and the PL spectrum was analyzed by a high-resolution spectrometer (SP 2500i, Princeton). X-ray diffractometer (Siemens D5005) was used to analyze the crystalline structures of the material. The Raman shifts of the samples were investigated by Raman spectroscopy (Labram Hr800, Horiba)

2.4. Antibacterial and Antifungal Property Investigation of the Materials

We chose *E. coli* and *C. albicans* which represent bacteria and fungi for the test. The cultured medium for *E. coli* is nutrient broth, and for *C. albicans* is YEPD broth [28]. Firstly, we poured 10 mL medium of each microbe into flasks. The starting density of *E. coli* and *C. albicans* was $(1.1\pm0.2)\times10^5$ and $(4.5\pm0.4)\times10^4$ CFU/mL, respectively. In each test, three sample groups including an untreated control group, a group treated with a P0 sample, and a last group treated with a PZn sample were prepared. Afterward, we incubated the samples at 37 ℃ for 24 hours and repeated the test 3 times. Finally, we determined optical density (OD) at 600 nm wavelength by using a spectrophotometer (Helios Epsilon, Thermo Spectronic). The growth inhibition of each sample can be estimated by the following formula:

$R(\%) = \frac{(OD_{control} - OD_{treated})}{OD_{control}}$ [18], where is growth inhibition in percent, $OD_{control}$ is the OD value of the control sample, and is OD value of the sample treated by the materials.

3. Result and Discussion

3.1. Characteristics of As-Synthesized Zinc-Modified Paper

Figure 1 indicates the XRD patterns of the samples P0 and PZn. It can be easily noticed that in the XRD pattern of the P0 sample (Figure 1a), the first two peaks at 15.48° and 22.40° (marked as asterisks) are the characteristic peaks of cellulose I [19, 20]. The other peaks (marked as diamond) correspond to the lattices of calcite ($CaCO_3$) that are usually used as a filler in commercial paper products [21]. Figure 1b represents the XRD patterns of PZn. The two peaks of cellulose can be observed, which proves that the hydrothermal process did not create any significant influence on the cellulose lattice structure. However, the peaks of calcite were replaced by several new peaks at 12.81°, 27.90°, 30.69°, 32.70°, 34.65°, and 35.64° referred to the phase of hydrozincite ($Zn_5(OH)_6(CO_3)_2$) [22–25]. The corresponding Miller's indices of these peaks are (200), (020), (311), (401), (-221), and (510), respectively. The absence of calcite peaks together with the appearance of hydrozincite characteristic peaks proves that during the synthesizing process the chemical interaction between calcite and zinc ions generated hydrozincite. This finding is also a good agreement with previous works [22-25].

As indicated in Figure 1c, the PL spectrum of the P0 sample has a high-intensity emission peak at 438 nm because of the appearance of gelatin [26] and cellulose fibers [27]. As seen in the figure, the PL spectrum of the PZn sample demonstrates a significantly lower intensity at 438 nm than that of the P0 sample by a factor of 1.5. The decrease in PZn's PL spectra compared to P0 can be attributed to several factors. Hydrozincite, as referenced in the study [28], has high absorbance in the 200-500 nm range, which covers the excitation wavelength and the PL emission range of the commercial paper (325 nm and 400-500 nm, respectively).

When the hydrozincite nanostructure was grown on the paper's surface, it absorbed a portion of the excitation beam. This led to a reduction of the energy available for the paper's PL emission. Additionally, hydrozincite also absorbed the paper's PL emission, further decreasing the observed intensity. Moreover, the emission in the shorter wavelength of hydrozincite (350-400 nm) resulted in a slight blue shift in PZn's spectrum. These again confirm the successful implementation of Zn^{2+} ions on the surface of the commercial paper.

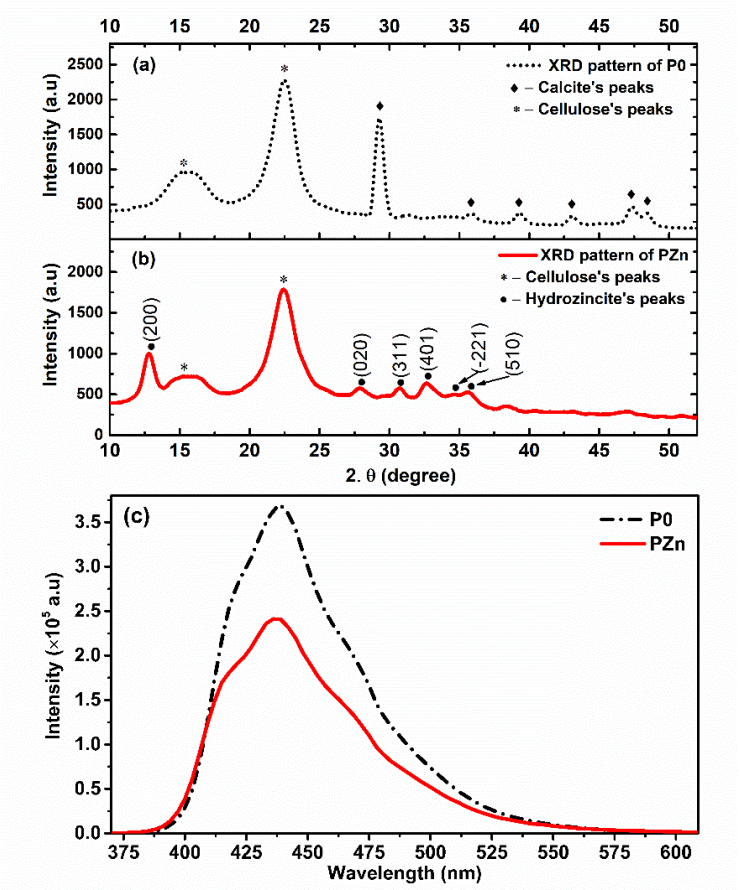

Figure 1. XRD patterns of the (a) P0 sample and (b) PZn sample, (c,d) PL spectrum of P0 and PZn samples.

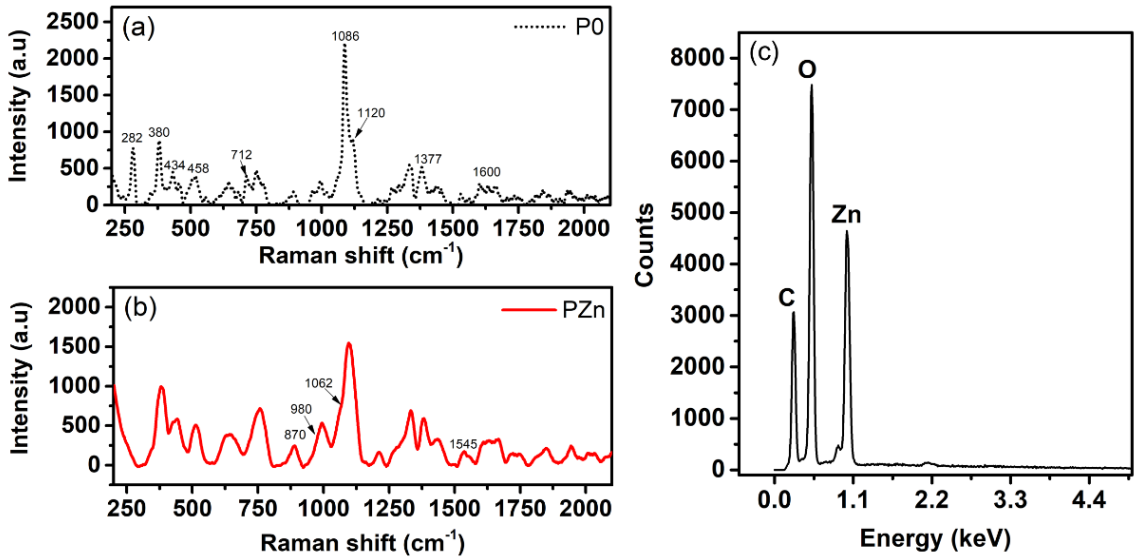

Figure 2. Raman shift of (a) P0 sample (b) PZn sample, and (c) EDS spectrum of the PZn sample.

Figure 2 represents the Raman shifts of P0 and PZn samples. As seen in Figure 2a, the Raman shift of the P0 indicates the specific bands of cellulose. The region of 375-550 cm^{-1} is attributed to the C-C-C, C-O-C, O-C-C, and O-C-O bending modes [29]. The region in range from 1095 to 1120 cm^{-1} refers to the C-O-C stretching symmetric, and the band around 1377 cm^{-1} corresponds to the H-C-H, H-C-C, H-O-C, and C-O-H bending [29]. Moreover, the Raman shift of the P0 sample also displays the instinct bands of calcite crystals [30]. These bands include several peaks at 1086, 712, and 282 cm^{-1}, which are related to the stretching mode of carbonate ions (CO_3^{2-}), the bending modes of carbonate ions, and the translational and rotational lattice modes, respectively. The band shifts around 1600 cm^{-1} are relevant to lignin groups. The Raman shift of the PZn samples is shown in Figure 2b. Besides some band shifts from the bare paper sheets, we can observe some new featured band shifts at around 1062 and 879 cm^{-1}. They are relevant to the vibration of CO_3^{2-} ions in hydrozincite [31]. The others were 980 and 1545 cm^{-1} which correspond to the deformation of OH^- ions and CO_3^{2-} ions in the hydrozincite crystals [23, 31]. The appearance of characteristic band shift of hydrozincite crystals again confirms the successful growth of hydrozincite on the commercial paper sheet.

The formation of hydrozincite on the paper sheets could be explained by the calcite crystals' absorbance of Zn^{2+} ions in the aqueous medium. In this process, the absorbed Zn^{2+} ion replaced Ca^{2+} ions on the surface of paper to form hydrozincite nanostructures [32]. The ion exchange process was confirmed by the EDS spectrum of the PZn sample in Figure 2c, showing characteristic peaks of carbon, oxygen, and zinc at energy levels of 0.27, 0.52, and 1.01 keV. The PZn sample contained 8.03% zinc atoms, as indicated in Table 1. The absence of calcium peaks in the EDS spectrum indicates that the ion exchange process between Zn^{2+} and Ca^{2+} was completed, resulting in the formation of hydrozincite in the PZn sample.

Table 1. Atomic density of elements in a PZn sample

Elements	Atomic density
C	47.56 %
O	44.41 %
Zn	8.03 %

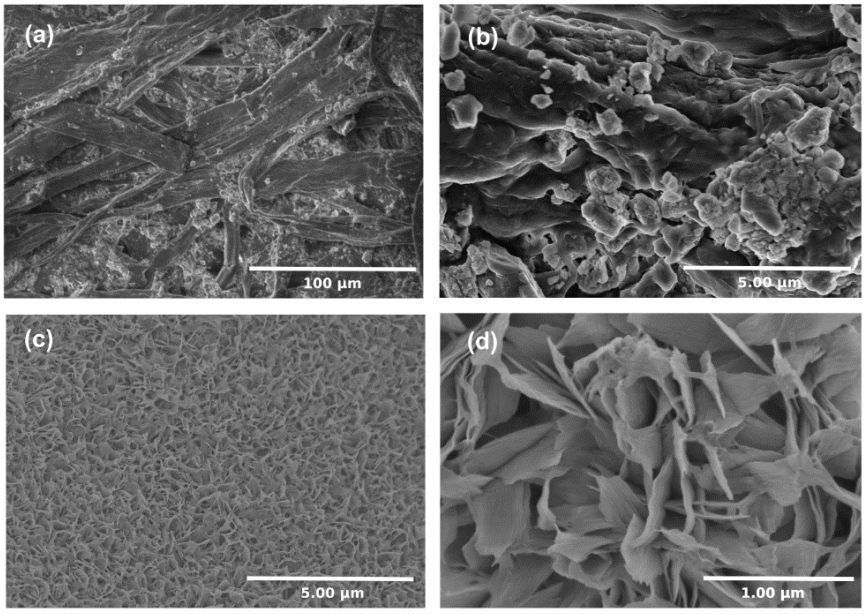

Figure 3. SEM images of (a-b) P0 sample and (c-d) PZn sample.

Figure 3 shows the SEM images of bare paper (P0) and hydrozincite nanostructure synthesized on paper (PZn). The surface morphology of the P0 sample demonstrates a bunch of cellulose fibers with variable diameters. On top of the fiber, a cluster of large grains is also observed which is referred to as calcite crystals. Interestingly, for the PZn, the whole surface is entirely covered by the flake shape structures of hydrozincite (Figure 3c, d). The size of the hydrozincite nanoflakes is approximately 422 ± 89 nm in diameter. Due to the high density and even distribution of the nanoflake structures, the materials can easily contact with the microbial cells. Furthermore, the nanoflake morphology of the PZn contains sharp edges and spikes which can damage the microorganisms. These fostered the antibacterial and antifungal properties of the nanomaterials. We will discuss more in detail in the next part.

3.2. Antibacterial and Antifungal Activities Test

Figure 4 illustrates the results of the antibacterial and antifungal tests. The starting density of bacteria and fungi was in order of 10^5 and 10^4 CFU/mL, respectively. After 24 hours of growing, the OD600 value of control samples became significant at 1.203±0.052 for *E. coli* and 1.667±0.108 for *C. albicans*. In fact, at that time, the population of the microorganisms was saturated, which led to the large value of the OD600. For the P0 samples, similar results were also observed, which demonstrated that the bare paper sheets used in this study are highly biocompatible and did not cause any damage to the living organisms. The differences only came from the group with PZn treatment. When tested against *C. albicans*, the PZn samples were able to reduce the OD600 value (a measure of microbial growth) by almost half compared to the control sample after 24 hours. This indicates a growth inhibition of 52.14% for *C. albicans*, highlighting the effective antifungal properties of the PZn material. Moreover, when exposed to *E. coli*, the PZn samples resulted in an OD600 value of approximately 0, indicating that the bacterial population was almost entirely inhibited. This corresponds to a remarkable growth inhibition rate of 98.95% for *E. coli*, indicating strong antibacterial activity of the PZn material. These findings confirm that the PZn samples possess potent antibacterial and antifungal properties, making them highly effective in inhibiting the growth and development of *C. albicans* and *E. coli*. Such promising results further emphasize the potential of PZn as a valuable component in the development of antibacterial and antifungal packaging materials for food preservation and safety.

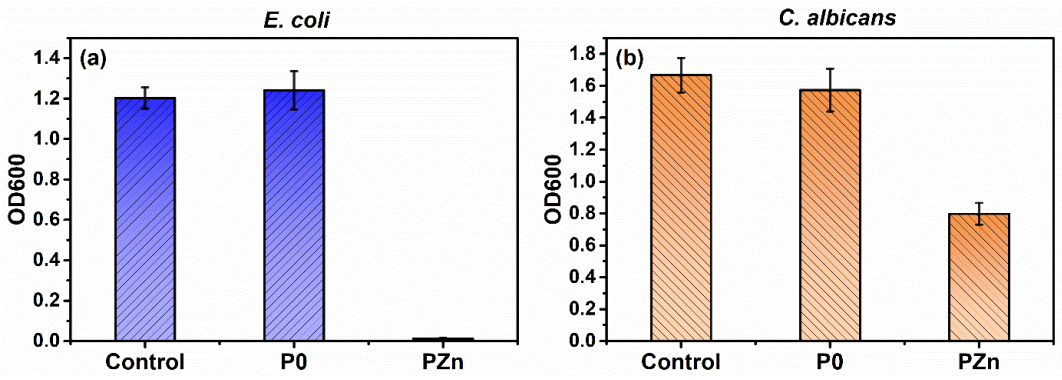

Figure 4. OD value of (a) *E. coli*, and (b) *C. albicans* (Control- untreated group, P0- group treated by blank paper sheets, and PZn-group treated by Zn-modified paper sheets) after 24 hours of growth).

The antibacterial and antifungal properties of hydrozincite nanomaterial were not comprehensively reported. In these works, we propose that the mechanism behind the antibacterial and fungal effects is the dispensation of Zn^{2+} ions from the hydrozincite nanomaterial into the liquid medium [33]. Note that, hydrozincite is well known as a quite stable material in ambient air and neutral to alkaline conditions, but it can be dissolved in acidic solutions [34]. However, when microorganisms are introduced into the medium. Their metabolic activities can create an acidic environment [35-38], leading to erosion of the hydrozincite structure and subsequent release of Zn^{2+} ions. As a result, Zn^{2+} ions can be released from the hydrozincite, thus, passing through the cell membrane, and finally causing damage to the organelles [39]. The conditional release of Zn^{2+} ions paves the future applications of PZn materials not only for antimicrobial applications but also for future biological and medical applications.

4. Conclusion

We have successfully implanted Zn^{2+} ions on commercial paper sheets by using an economical hydrothermal technique. The XRD patterns, the PL spectrum, and the SEM images of the PZn demonstrated that the hydrozincite nanoflakes were successfully grown on the commercial paper sheets with high quality. The results of the antibacterial and antifungal test showed that the PZn sheets have antibacterial and antifungal activities, especially strong inhibition against *E. coli*. The remarkable antimicrobial properties of the PZn were attributed to the conditional release of Zn^{2+} ion from the hydrozincite nanoflakes, and due to the notable nanoflake morphology of the PZn. Along with the eco-friendliness, and the biocompatibility of the paper substrate, the Zn-implanted paper sheets showed a high potential application in food packing.

Acknowledgements

This work was supported by the National Foundation for Science and Technology Development (NAFOSTED) of Vietnam through Grant No 103.03-2019.315.

References

[1] S. Y. Sung, L. T. Sin, T. T. Tee, S. T. Bee, A. R. Rahmat, W. A. Rahman, A. C. Tan, M. Vikhraman, Antimicrobial Agents for Food Packaging Applications, Trends Food Sci Technol, Vol. 33, No. 2, 2013, pp. 110-123, https://doi.org/10.1016/j.tifs.2013.08.001.

[2] X. Sun, J. Wang, M. Dong, H. Zhang, L. Li, L. Wang, Food Spoilage, Bioactive Food Fresh-Keeping Films and Functional Edible Coatings: Research Status, Existing Problems And Development Trend, Trends Food Sci Technol, Vol. 119, 2022, pp. 122-132, https://doi.org/10.1016/j.tifs.2021.12.004.

[3] T. Huang, Y. Qian, J. Wei, C. Zhou, Polymeric Antimicrobial Food Packaging and Its Applications, Polymers (Basel), Vol. 11, No. 3, 2019, pp. 560, https://doi.org/10.3390/polym11030560.

[4] S. Mangaraj, A. T. Goswami, A. V. Mahajan, Applications of Plastic Films for Modified Atmosphere Packaging of Fruits and Vegetables: A Review, Food Eng Rev, Vol. 1, No. 2, 2009, pp. 133-158, https://doi.org/10.1007/s12393-009-9007-3.

[5] A. Sonia, K. P. Dasan, Celluloses Microfibers (CMF)/Poly (Ethylene-Co-Vinyl Acetate) (EVA) Composites for Food Packaging Applications: a Study Based on Barrier and Biodegradation Behavior, J. Food Eng, Vol. 118, No. 1, 2013, pp. 78-89, https://doi.org/10.1016/j.jfoodeng.2013.03.020.

[6] A. Kanavouras, P. H. Munoz, F. A. Coutelieris, Packaging of Olive Oil: Quality Issues and Shelf Life Predictions, Food Rev Int, Vol. 22, No. 4, 2007, pp. 381-404, https://doi.org/10.1080/87559120600865149.

[7] T. Heinze, O. A, El Seoud, A. Koschella, Production and Characteristics of Cellulose from Different Sources, In Cellul. Deriv. Springer, Cham, 2018, pp 1-38, https://doi.org/10.1007/978-3-319-73168-1_1.

[8] P. Gao, R. Cha, H. Luo, Y. Xu, P. Zhang, L. Han, X. Wang, Z. Zhang, X. Jiang, Development of

Antimicrobial Oxidized Cellulose Film for Active Food Packaging, Carbohydr Polym, Vol. 278, 2022, pp. 118922, https://doi.org/10.1016/j.carbpol.2021.118922.

[9] M. A. Tartanson, L. Soussan, M. Rivallin, S. Pecastaings, C. V. Chis, D. Penaranda, C. Roques, C. Faur, Dynamic Mechanisms of The Bactericidal Action of An Al_2O_3-TiO_2-Ag Granular Material on An Escherichia Coli Strain, Appl Environ Microbiol, Vol. 81, No. 20, 2015, pp. 7135-7142, https://doi.org/10.1128/aem.01950-15.

[10] H. J. Park, J. Y. Kim, J. Kim, J. H. Lee, J. S. Hahn, M. B. Gu, J. Yoon, Silver-Ion-Mediated Reactive Oxygen Species Generation Affecting Bactericidal Activity, Water Res, Vol. 43, No. 4, 2009, pp. 1027-1032, https://doi.org/10.1016/j.watres.2008.12.002.

[11] R. Arif, P. S. Nayab, I. A. Ansari, M. Shahid, M. Irfan, S. Alam, M. Abid, Rahisuddin, Synthesis, Molecular Docking and DNA Binding Studies of Phthalimide-Based Copper(II) Complex: In Vitro Antibacterial, Hemolytic and Antioxidant Assessment, J. Mol Struct, Vol. 1160, 2018, pp. 142-153, https://doi.org/10.1016/j.molstruc.2018.02.008.

[12] Y. Kaneko, M. Thoendel, O. Olakanmi, B. E. Britigan, P. K. Singh, The Transition Metal Gallium Disrupts Pseudomonas Aeruginosa Iron Metabolism and Has Antimicrobial and Antibiofilm Activity, J Clin Invest, Vol. 117, No. 4, 2007, pp. 877-888, https://doi.org/10.1172/jci30783.

[13] S. C. Cunnane, Zinc: Clinical and Biochemical Significance, CRC Press, Boca Raton, 2018, https://doi.org/10.1201/9781351077811.

[14] R. Sl Yamgar, Y. Nivid, S. Nalawade, M. Mandewale, R. G. Atram, S. S. Sawant, Novel Zinc(II) Complexes of Heterocyclic Ligands as Antimicrobial Agents: Synthesis, Characterisation, and Antimicrobial Studies, Bioinorg. Chem. Appl, 2014. https://doi.org/10.1155/2014/276598

[15] I. Sheikhshoaie, N. Lotfi, J. Sieler, H. Krautscheid, M. Khaleghi, Synthesis, Structures and Antimicrobial Activities Of Nickel(II) and Zinc(II) Diaminomaleonitrile-Based Complexes, Transit Met Chem, Vol. 43, No. 6, 2018, pp. 555-562, https://doi.org/10.1007/s11243-018-0241-5.

[16] A. M. Youssef, S. M. E. Sayed, H. S. E. Sayed, H. H. Salama, A. Dufresne, Enhancement of Egyptian Soft White Cheese Shelf Life Using A Novel Chitosan/Carboxymethyl Cellulose/Zinc Oxide Bionanocomposite Film, Carbohydr Polym, Vol. 151, 2016, pp. 9-19, https://doi.org/10.1016/j.carbpol.2016.05.023.

[17] J. Shojaeiarani, A. Shirzadifar, C. Shine, A. M. Reisi, Hybrid Nanocomposite Packaging Films from Cellulose Nanocrystals, Zinc Sulfide Quantum Dots Reinforced Polylactic Acid with Fluorescent and Antibacterial Properties, Polym Eng Sci, Vol. 62, No. 5, 2022, pp. 1562-1570, https://doi.org/10.1002/pen.25944.

[18] S. Sarwar, S. Chakraborti, S. Bera, I. A. Sheikh, K. M. Hoque, P. Chakrabarti, The Antimicrobial Activity of Zno Nanoparticles Against Vibrio Cholerae: Variation In Response Depends on Biotype, Nanomedicine Nanotechnology, Biol Med, Vol. 12, No. 6, 2016, pp. 1499-1509, https://doi.org/10.1016/j.nano.2016.02.006.

[19] M. Dasari, P. R. Rajasekaran, R. Iyer, P. Kohli, Calligraphic Solar Cells: Acknowledging Paper and Pencil, J. Mater Res, Vol. 31, No. 17, 2016, pp. 2578-2589, https://doi.org/10.1557/jmr.2016.281.

[20] L. Jiao, J. Ma, H. Dai, Preparation and Characterization of Self-Reinforced Antibacterial and Oil-Resistant Paper using a Naoh/Urea/Zno Solution, PLoS One, Vol. 10, No. 10, 2015, pp. e0140603, https://doi.org/10.1371/journal.pone.0140603.

[21] O. A. Jimoh, K. S. Ariffin, H. B. Hussin, A. E. Temitope, Synthesis of Precipitated Calcium Carbonate: A Review, Carbonates and Evaporites, Vol. 33, No. 2, 2017, pp. 331-346, https://doi.org/10.1007/s13146-017-0341-x.

[22] M. Y. Nassar, M. M. Moustafa, M. M. Taha, Hydrothermal Tuning of The Morphology and Particle Size of Hydrozincite Nanoparticles Using Different Counterions to Produce Nanosized Zno as An Efficient Adsorbent for Textile Dye Removal, RSC Adv, Vol. 6, No. 48, 2016, pp. 42180-42195, https://doi.org/10.1039/c6ra04855b.

[23] M. C. Hales, R. L. Frost, Synthesis and Vibrational Spectroscopic Characterisation of Synthetic Hydrozincite and Smithsonite, Polyhedron, Vol. 26, No. 17, 2007, pp. 4955-4962, https://doi.org/10.1016/j.poly.2007.07.002.

[24] P. Lattanzi, C. Maurizio, C. Meneghini, G. Giudici de, F. Podda, Uptake of Cd in Hydrozincite, $Zn_5(CO_3)_2(OH)_6$: Evidence from X-Ray Absorption Spectroscopy and Anomalous

X-Ray Diffraction, Eur J Mineral, Vol. 22, No. 4, 2010, pp. 557-564, https://doi.org/10.1127/0935-1221/2010/0022-2053.

[25] F. Podda, P. Zuddas, A. Minacci, M. Pepi, F. Baldi, Heavy Metal Coprecipitation with Hydrozincite [Zn5(CO3)2(OH)6] from Mine Waters Caused by Photosynthetic Microorganisms, Appl Environ Microbiol, Vol. 66, No. 11, 2000, pp. 5092-5098, https://doi.org/10.1128/aem.66.11.5092-5098.2000.

[26] C. G. Cole, J. J. Roberts, The Fluorescence of Gelatin and Its Implications, Imaging Sci J, Vol. 45, No. 3-4, 1997, pp. 145-149, https://doi.org/10.1080/13682199.1997.11736396.

[27] Y. W. Zhang, Y. Zhang, Nonconventional Macromolecular Luminogens with Aggregation-Induced Emission Characteristics, J. Polym Sci Part A Polym Chem, Vol. 55, No. 4, 2017, pp. 560-574, https://doi.org/10.1002/pola.28420.

[28] E. Turianicová, M. Kaňuchová, A. Zorkovská, M. Holub, Z. Bujňáková, E. Dutková, M. Baláž, L. Findoráková, M. Balintová, A. Obut, CO2 Utilization for Fast Preparation of Nanocrystalline Hydrozincite, J. CO2 Util, Vol. 16, 2016, pp. 328-335, https://doi.org/10.1016/j.jcou.2016.08.007.

[29] M. S. Chargot, J. Cybulska, A. Zdunek, Sensing The Structural Differences in Cellulose from Apple and Bacterial Cell Wall Materials by Raman and FT-IR Spectroscopy, Sensors, Vol. 11, No. 6, 2011, pp. 5543-5560, https://doi.org/10.3390/s110605543.

[30] F. C. Donnelly, F. P. Milton, V. Framont, O. Cleary, P. W. Dunne, Y. K. Gun'ko, Synthesis of $CaCO_3$ Nano- and Micro-Particles by Dry Ice Carbonation, Chem Commun, Vol. 53, No. 49, 2017, pp. 6657-6660, https://doi.org/10.1039/c7cc01420a.

[31] M. C. Hales, R. L. Frost, Thermal Analysis of Smithsonite and Hydrozincite, J. Therm Anal Calorim, Vol. 91, No. 3, 2008, pp. 855-860, https://doi.org/10.1007/s10973-007-8571-0.

[32] J. M. Zachara, J. A. Kittrick, J. B. Harsh, The Mechanism of Zn^{2+} Adsorption on Calcite, Geochim Cosmochim Acta, Vol. 52, No. 9, 1988, pp. 2281-2291, https://doi.org/10.1016/0016-7037(88)90130-5.

[33] N. Radovanovic, I. Malagurski, S. Levic, A. Nesic, G. C. Barjas, A. Kalusevic, V. Nedovic, V. Pavlovic, S. D. Brankovic, Influence of Different Concentrations of Zn-Carbonate Phase on Physical-Chemical Properties of Antimicrobial Agar Composite Films, Mater Lett, Vol. 255, 2019, pp. 126572, https://doi.org/10.1016/j.matlet.2019.126572.

[34] A. K. Alwan, P. A. Williams, Mineral Formation from Aqueous Solution, Part I. The Deposition of Hydrozincite, $Zn_5(OH)_6(CO_3)_2$, from Natural Waters, Transit Met Chem, Vol. 4, No. 2, 1979, pp. 128-132, https://doi.org/10.1007/bf00618840.

[35] F. V. Gambacorta, J. J. Dietrich, Q. Yan, B. F. Pfleger, Rewiring Yeast Metabolism to Synthesize Products Beyond Ethanol, Curr Opin Chem Biol, Vol. 59, 2020, pp. 182-192, https://doi.org/10.1016/j.cbpa.2020.08.005.

[36] E. Stewart, S. Hawser, N. A. Gow, Changes in Internal and External pH Accompanying Growth of Candida Albicans: Studies Of Non-Dimorphic Variants, Arch Microbiol, Vol. 151, No. 2, 1989, pp. 149-153, https://doi.org/10.1007/bf00414430/metrics.

[37] R. S. Clemente, M. I. Igeño, A. G. Población, M. I. Guijo, F. Merchán, R. Blasco, Study of pH Changes in Media during Bacterial Growth of Several Environmental Strains, Proc 2018, Vol. 2, No. 20, 2018, pp. 1297, https://doi.org/10.3390/proceedings2201297.

[38] D. A. Hodgson, Primary Metabolism and Its Control in Streptomycetes: A Most Unusual Group of Bacteria, Adv Microb Physiol, Vol. 42, 2000, pp. 47-238, https://doi.org/10.1016/s0065-2911(00)42003-5.

[39] A. Sirelkhatim, S. Mahmud, A. Seeni, N. H. Kaus, L. C. Ann, S. K. Bakhori, H. Hasan, D. Mohamad, Review on Zinc Oxide Nanoparticles: Antibacterial Activity and Toxicity Mechanism, Nano-Micro Lett, Vol. 7, No. 3, 2015, pp. 219, https://doi.org/10.1007/s40820-015-0040-x.